

Accelerated growth by flash heating of high critical current Trifluoroacetate solution derived epitaxial superconducting YBa₂Cu₃O₇ films

Ziliang Li, Mariona Coll, Bernat Mundet, Anna Palau, Teresa Puig, Xavier Obradors*

Institut de Ciència de Materials de Barcelona, CSIC

Campus de la UAB, 08193 Bellaterra, Catalonia, Spain

The influence of water supply

The temperature where the humid atmosphere is initiated and the waiting time remaining in dry conditions are very important processing parameters because they influence the precursor film porosity and hence the growth of YBCO and the final microstructure of the films. Here we report an analysis of this issue in the flash heating process in order to select the optimal conditions to growth high critical current YBCO films. The films investigated here were grown at 810 °C after flash heating, the water supply was initiated at 20 °C, 110 °C or 810 °C. In the last case it was tested as well the influence of waiting in dry atmosphere during 5 min. The microstructure and the superconducting properties of all these films were investigated.

Figure S1 shows a set of cross-sectional FIB images which provide information about the porosity evolution of the as-pyrolyzed film and the films quenched from the different thermal processing steps mentioned before. The FIB cross-sectional image of the conventional, as-pyrolyzed YBCO film, evidences the formation of a vertical open porosity which can be attributed to the poor mechanical properties of the films during this stage¹ and a fast gas escape toward the film surface associated with the high kinetics of the decomposition process.² Notice that the density of these pores is significantly decreased during the flash heating process to the growth temperature; see Figure S1 (b)-(d). It is remarkable to note that the inner pores in the film quenched from 810 °C in humid gas atmosphere without annealing are almost completely absent; see Figure S1 (b). Whereas, there are still some pores remaining at the film-substrate interface for films quenched from 810 °C in dry gas atmosphere without annealing (Figure S1 (c)), the film can be completely compacted after annealing for 5 min (Figure S1 (d)). The film thicknesses are estimated to be 260 nm, 320 nm and 270 nm for films quenched from dry gas atmosphere after annealing 0 min, humid gas atmosphere after annealing 0 min and humid gas atmosphere after annealing 5 min, respectively. All of them exhibit a strong shrinkage from the as-pyrolyzed YBCO precursor film (450 nm). These observations are of great importance to illustrate that the densification process starts during the thermal heating process, before YBCO nucleation and growth. It is

concluded, therefore, that the application of the FH process is beneficial to minimize the film porosity prior to the YBCO nuclei appear, ensuring a continuous atomic diffusion at the YBCO nucleation and growth stages. On the other hand, the vertical open pores are necessary to the water diffusion to the heterogeneous nucleation sites of YBCO to some extent. Taking these two conflicting requirements into account, it is clear that some further optimizations should be achieved to obtain highly dense epitaxial YBCO coated conductors. Therefore, further works towards the achievement of high microstructural and superconducting properties will be illustrated in the next two sections.

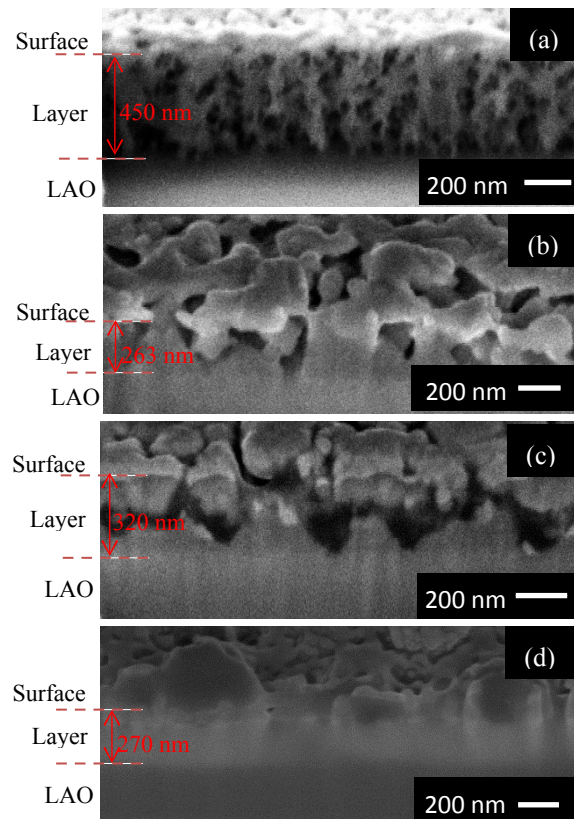


Figure S1. FIB images of (a) as-pyrolyzed YBCO and YBCO thin films quenched from (b) 810 °C and humid gas atmosphere without thermal annealing ($t=0$); (c) 810 °C and dry gas atmosphere without annealing; (d) 810 °C and dry gas atmosphere after annealing for 5 min.

Figure S2 (a)-(b) present SEM images of the YBCO thin films grown from the FH process with diverse two supply temperatures (110 °C and 810 °C). The observation indicates that highly c-oriented and homogeneous YBCO thin films can be obtained when H₂O is introduced at 110-810 °C without dwell time. XRD θ -2 θ scans have been carried out systematically on the YBCO thin films with water supply at 110-810 °C, as typically shown in Figure S2 (c). These x-ray diffraction frames display typical epitaxially grown YBCO features. On the other hand, the crystalline perfection of the epitaxial YBCO thin films (i.e. films 110 °C-0 min, 720 °C-0 min and 810 °C-0 min) has been investigated by estimating the FWHM of the Bragg peaks using XRD ω -scans and ϕ -scans for (005) and (103) YBCO peaks,

respectively. Figure S2 (d) presents the rocking curve of the YBCO (005) for all the epitaxial YBCO thin films. The estimated $\Delta\omega$ values show a gradual increase from $\sim 0.6^\circ$ for film 110 °C-0 min to 0.8° for film 810 °C-0 min. While the film 110 °C-0 min presents a $\Delta\phi$ value of $\sim 1.3^\circ$. It is clear that the film 110 °C-0 min presents good out-of-plane and in-plane texture quality, which is comparable with YBCO films grown from the CTA process ($\Delta\omega = \sim 0.5^\circ$ and $\Delta\phi = \sim 1.2^\circ$). Moreover, the c-parameter for all the epitaxial FH films are estimated to be $11.692 \pm 0.003 \text{ \AA}$, which is very similar to the CTA films ($11.689 \pm 0.002 \text{ \AA}$).

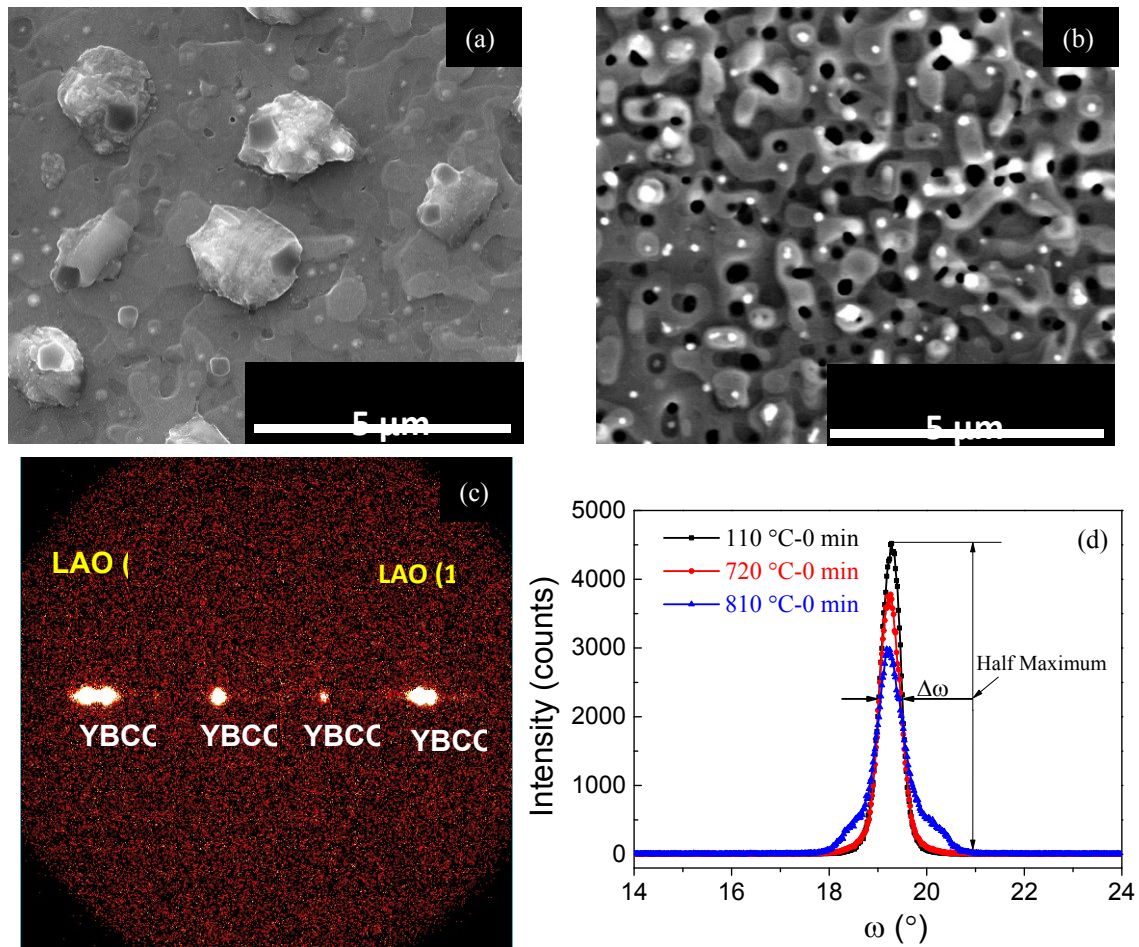


Figure S2. (a)-(b) SEM micrographs of YBCO thin films grown from the FH process with water introduction at (a) 110 °C-0 min and (b) 810 °C-0 min; (c) typical two dimensional XRD frames of YBCO thin films grown from the FH process with water supply at 110 – 810 °C; (d) rocking curves of the (005) YBCO diffraction peak for films 110 °C-0 min, 740 °C-0 min and 810 °C-0 min, respectively.

SEM micrographs of the YBCO film 810 °C-5 min indicate that randomly oriented YBCO grains, i.e. (103) oriented YBCO grain (see Figure S3 (a)), formed during the growth process. It is noteworthy that there is an extra diffraction ring appearing at $2\theta = 32.8^\circ$ for films 810 °C-

5 min, indexed as corresponding to the (103) Bragg peak of YBCO and indicates that some randomly oriented grains have been found.

We attribute the degradation of the film texture quality to an excessive supersaturation s (see equation S1) during nucleation.

Classical nucleation theory establishes that the nucleation process of epitaxial YBCO islands occurs when the energy of first nuclei overcome their energy barriers ΔG^* , described in Equation 1-1 in the main text. A detailed analysis (see section 1.2.2.1) of the relationship between this energy barrier ΔG^* and $|\Delta\mu|$ predicted that c-axis grains are prone to nucleate under low $|\Delta\mu|$, while a/b-axis and randomly oriented nuclei appear at high $|\Delta\mu|$. The nucleation events of YBCO thin films can be safely explained by this analysis when precursor film has a good permeability. However, the influence of gas diffusion issues on the nucleation energy should be taken into account when the gas impedance appears. In this scenario, Solovyov et al^{3,4} extended the schema established based on the classical nucleation theory to a collective effect in the nucleation events taking into account the influence of the gas impedance. In low film permeability systems (i.e. thick or dense films), it is predicted that there exists high surface energy sites which are influenced by the already existing stable nuclei. These sites provide areas with high energy barriers thus retarding nucleation events. The supersaturation degrees (or driving force) of these sites could then be correlated with several processing parameters:

$$s = \frac{\Delta\mu}{kT} \propto \frac{dr}{P(H_2O)^{1/2} D_s} \quad \text{Equation S1}$$

where d is the film thickness, r the growth rate and D_s the HF diffusion permeability through the film precursor. From Equation S1, it is clearly seen that s is directly influenced by the gas (H_2O and HF) transfer through the YBCO precursor layer.⁵ As it has been shown in the previous FIB studies, the precursor layer is gradually densified during the annealing processes; see Figure S1 (b)-(d). The densification of these precursor layers could decrease the film permeability (D_s) and/or $P(H_2O)$. This effect could increase the $|\Delta\mu|$, leading to the formation of a-axis or randomly oriented grains and, consequently, damage the growth uniformity of the epitaxy. Therefore, an earlier introduction of H_2O vapour is required in order to ensure high

permeability for gas diffusion through the film during the nucleation and growth process of YBCO films.

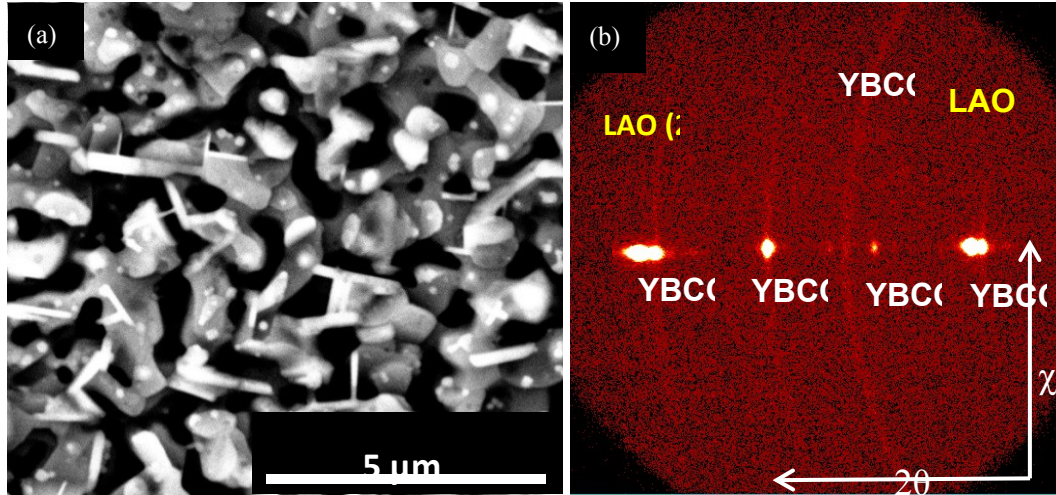


Figure S3. (a) SEM micrograph and (b) GADDS frame of YBCO thin film grown from the FH (810 °C) process with water supply at 810 °C after annealed for 5 min.

Figure S4 (a) displays several superconducting properties, including the onset superconducting transition temperature (T_c^{onset}), transition width (ΔT_c) and self-field critical current (J_c^{sf}) measured at 5K and 77K. The T_c^{onset} and ΔT_c values of the epitaxially grown YBCO thin films are $\sim 88.5 \pm 0.5$ K and $\sim 7.5 \pm 3.0$ K, respectively. Besides, both $J_c^{sf}(5K)$ and $J_c^{sf}(77K)$ show similar evolution trend with water introduction time, as observed from the J_c evolution plots shown in Figure S4 (a). Note that YBCO thin film 110 °C-0 min presents the highest $J_c^{sf}(5K)$ and $J_c^{sf}(77K)$ values, 28.9 MA/cm² and 3.2 MA/cm², respectively. A significant degradation of J_c s arise for films 20 °C-0 min and 810 °C-5 min, which is accounted for the current blocking effect due to the formation of large angle grain boundaries generated between c-axis and non-c-axis oriented YBCO grains.⁶ Moreover, a small reduction of J_c occurs in the epitaxial YBCO thin films following the increase of water opening temperature, i.e. films 110-810 °C-0 min.

Our results indicate, therefore, that the optimal temperature to initiate the humid atmosphere is 110 °C and so this is the process that was used to grow optimal YBCO films to disclose the influence of growth temperature on the final film defect structure and superconducting properties.

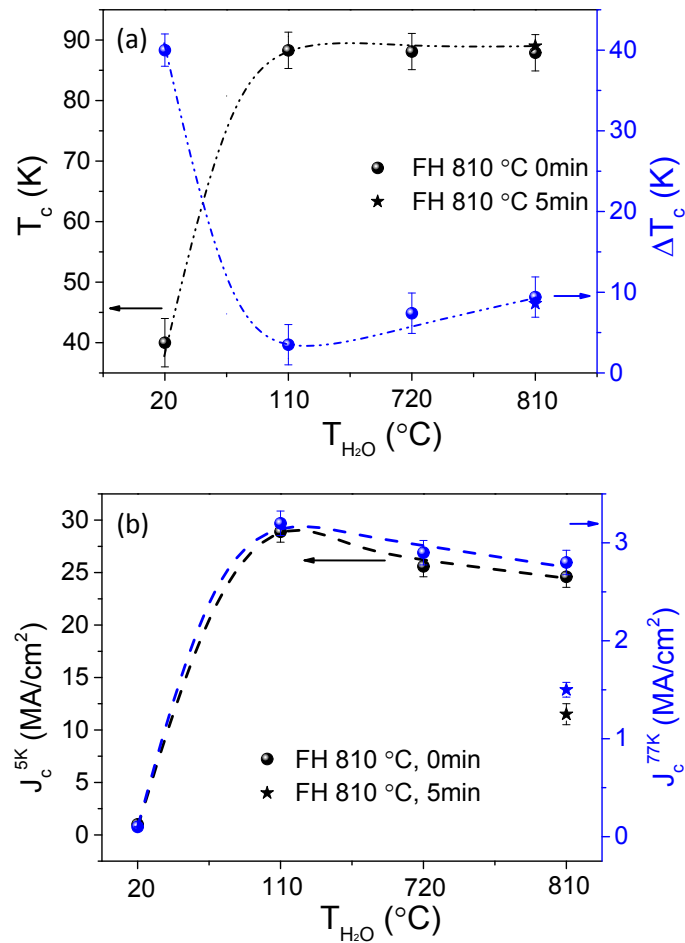


Figure S4. (a) Critical temperature (T_c) and transition width (ΔT_c) and (b) J_c obtained at 5K and 77K evolution determined inductively by SQUID measurement on the YBCO thin films grown from the FH (810 °C) growth process with different water introduction time.

References

1. X. Obradors, T. Puig, A. Pomar, F. Sandiumenge, N. Mestres, M. Coll, A. Cavallaro, N. Romà, J. Gázquez, J. C. González, O. Castaño, J. Gutierrez, A. Palau, K. Zalamova, S. Morlens, A. Hassini, M. Gibert, S. Ricart, J. M. Moretó, S. Piñol, D. Isfort and J. Bock, *Supercond. Sci. Technol.*, 2006, **19**, S13-S26.
2. A. Llordés, K. Zalamova, S. Ricart, A. Palau, A. Pomar, T. Puig, A. Hardy, M. K. Van Bael and X. Obradors, *Chem. Mater.*, 2010, **22**, 1686-1694.
3. V. F. Solovyov, H. J. Wiesmann and M. Suenaga, *Supercond. Sci. Technol.*, 2004, **18**, 239.
4. V. F. Solovyov, H. J. Wiesmann and M. Suenaga, *IEEE Trans. Appl. Supercond.*, 2005, **15**, 2739-2742.
5. C. Pop, B. Villarejo, F. Pino, B. Mundet, S. Ricart, M. de Palau, T. Puig and X. Obradors, *Supercond. Sci. Technol.*, 2019, **32**, 015004.
6. H. Hilgenkamp and J. Mannhart, *Rev. Mod. Phys.*, 2002, **74**, 485.